Temperature-independent carrier formation dynamics in bulk heterojunction

2015 Appl. Phys. Express 8 112301

(http://iopscience.iop.org/1882-0786/8/11/112301)

OPEN ACCESS

Applied Physics Express 8, 112301 (2015)

http://dx.doi.org/10.7567/APEX.8.112301

Temperature-independent carrier formation dynamics in bulk heterojunction

Kouhei Yonezawa[1], Takeshi Yasuda[2], and Yutaka Moritomo[1,3*]

[1]*Graduate School of Pure and Applied Science, University of Tsukuba, Tsukuba, Ibaraki 305-8577, Japan*
[2]*Photovoltaic Materials Unit, National Institute for Materials Science (NIMS), Tsukuba, Ibaraki 305-0047, Japan*
[3]*Center for Integrated Research in Fundamental Science and Engineering (CiRfSE), University of Tsukuba, Tsukuba, Ibaraki 305-8577, Japan*
E-mail: moritomo.yutaka.gf@u.tsukuba.ac.jp

Received August 27, 2015; accepted September 9, 2015; published online October 5, 2015

We investigated the effects of temperature on the carrier formation dynamics in a small-molecular blend film, 2,5-di-(2-ethylhexyl)-3,6-bis-(5″-*n*-hexy-[2,2′,5′,2″]terthiophen-5-yl)-pyrrolo[3,4-c]pyrrolo-1,4-dione (SMDPPEH)/[6,6]-phenyl C_{71}-butyric acid methyl ester ($PC_{71}BM$). We spectroscopically determined the absolute numbers of donor (n_{D^*}) and acceptor (n_{A^*}) excitons per absorbed photon as functions of the delay time (t), in addition to the relative number of donor carries (n_{D^+}). We found that the carrier formation dynamics is independent of temperature at 300 and 80 K: the carrier formation time ($\tau_{rise} = 0.4$ ps) is much faster than the decay time ($\tau_{decay} \approx 2.5$ ps) of donor excitons. The temperature independence strongly suggests that only excitons created near the donor–acceptor interface contribute to the carrier formation.

Organic solar cells (OSCs) with bulk heterojunctions (BHJs)[1,2] are promising energy conversion devices with flexibility. They have a low-cost production process, e.g., the roll-to-roll process. The BHJ active layer, which is usually sandwiched between a transparent indium tin oxide (ITO) anode and an Al cathode, consists of phase-separated nano-size domains of the donor (D) and acceptor (A) materials. In this layer, photo-irradiation creates donor (D^*) and acceptor (A^*) excitons within the respective nano domains. The photo-created excitons are considered to migrate to the D/A interface and separate into electrons and holes. Time-resolved spectroscopy is one of the most powerful tools for clarifying the carrier formation dynamics in BHJ layers.[3–14] The analyses of photo-induced absorption (PIA) reveal the *relative* numbers of excitons (D^* and A^*) and donor carriers (D^+) as functions of the delay time (t). For example, the spectroscopy revealed that the carrier formation time ($\tau_{rise} \approx 0.2$ ps) is comparable to the decay time ($\tau_{decay} \approx 0.3$ ps)[10] of A^* in poly[[4,8-bis[(2-ethylhexyl)oxy]-benzo[1,2-*b*:4,5-*b*′]dithiophene-2,6-diyl][3-fluoro-2-[(2-ethyl-hexyl)carbonyl]thieno[3,4-*b*]thiophenediyl]] (PTB7)/$PC_{71}BM$ blend film.[15–17]

The nano-size domain structure of the BHJ layers is advantageous for efficient charge formation and, in turn, high power-conversion efficiency (PCE). The complex domain structure of the BHJ layer, however, impedes the microscopic observation of the charge formation process. For example, scanning transmission X-ray microscopy (STXM) has revealed significant fullerene mixing within donor-rich domains.[18–20] In addition, Hedley et al.[21] reported sub-structures of ∼10 nm within the ∼100 nm domains in PTB7/$PC_{71}BM$ blend film. Here, we emphasize that the temperature effect provides significant clues on the charge formation process. For example, Moritomo et al.[22] reported that the carrier formation efficiency (Φ_{CF}), which is defined as the number of the photo-induced carriers per absorbed photon, is independent of temperature in regioregular poly(3-hexyl-thiophene) (rr-P3HT)/[6,6]-phenyl C_{61}-butyric acid methyl ester (PCBM) and PTB7/$PC_{71}BM$ blend films. The independence of temperature strongly suggests that the exciton dissociation should be treated using the quantum-mechanical wave-packet picture, rather than the Marcus theory,[23] in which the charge separation is governed by the displacement of surrounding molecules.

Among the donor materials, the oligothiophene-diketo-pyrrolopyrrole molecule with ethylhexyl substituents (SMDPPEH) is suitable for a detailed spectroscopic investigation on the charge formation dynamics because it shows intense and sharp PIAs due to D^* and D^+ in the infrared region.[12] In addition, the SMDPPEH/$PC_{71}BM$ BHJ solar cell shows a high PCE of 3.0%, reflecting the intense absorption of SMDPPEH for relatively long wavelengths.[24–26] In our previous paper,[12] we performed time-resolved spectroscopy in the SMDPPEH/$PC_{71}BM$ blend film at 300 K and derived the *relative* numbers of D^*, A^*, and D^+ as functions of t. However, the data points were too scattered to reveal the carrier formation dynamics in detail.

In this paper, we investigated the effects of temperature on the carrier formation dynamics in SMDPPEH/$PC_{71}BM$ blend film. By comparing the absolute intensities of the PIAs between the blend and neat films, we determined the *absolute* numbers of the donor (n_{D^*}) and acceptor (n_{A^*}) excitons per absorbed photon as functions of t. The improved data acquisition and analysis reveals that the carrier formation time ($\tau_{rise} = 0.4$ ps) is less than the decay times ($\tau_{decay} \approx 2.5$ ps) of D^*, indicating that the late decay component ($t \geq \tau_{rise}$) does not contribute to the carrier formation process. The independence of temperature and the low value of τ_{rise} strongly suggest that only the excitons created near the D/A interface contribute to the carrier formation process.

The SMDPPEH/$PC_{71}BM$ blend film was spin-coated on quartz substrates using a chlorobenzene solution of SMDPPEH:$PC_{71}BM$ of 1 : 1 by weight. Then, the blend film was dried in an inert N_2 atmosphere. SMDPPEH was purchased from Sigma-Aldrich and used as received. For comparison, we prepared spin-coated SMDPPEH ($PC_{71}BM$) films on quartz substrates using chlorobenzene (chloroform) solution. The thicknesses of the SMDPPEH neat, $PC_{71}BM$ neat, and SMDPPEH/$PC_{71}BM$ blend films were 39, 50, and 96 nm, respectively.

Time-resolved spectroscopy was performed in a pump–probe configuration at 300 and 80 K, the details of which are

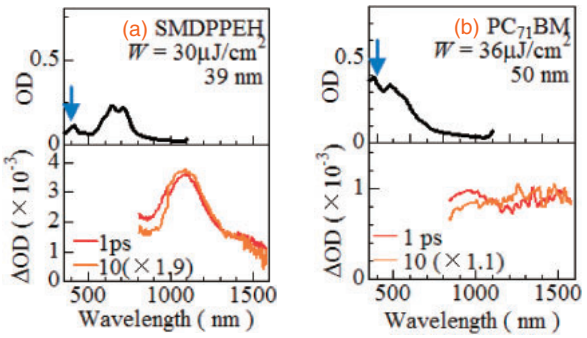

Fig. 1. Absorption (OD) spectra and differential absorption (ΔOD) spectra of (a) SMDPPEH and (b) $PC_{71}BM$ neat films at 300 K. Downward arrows indicate the excitation wavelengths. The data were replotted from Ref. 12.

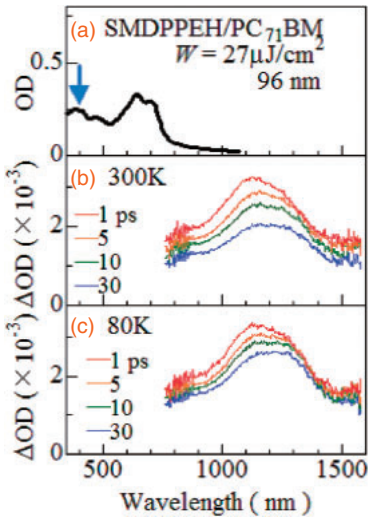

Fig. 2. (a) Absorption (OD) spectra SMDPPEH/$PC_{71}BM$ blend film at 300 K. Differential absorption (ΔOD) spectra of SMDPPEH/$PC_{71}BM$ blend films at (b) 300 K and (c) 80 K. A downward arrow in (a) indicates the excitation wavelength.

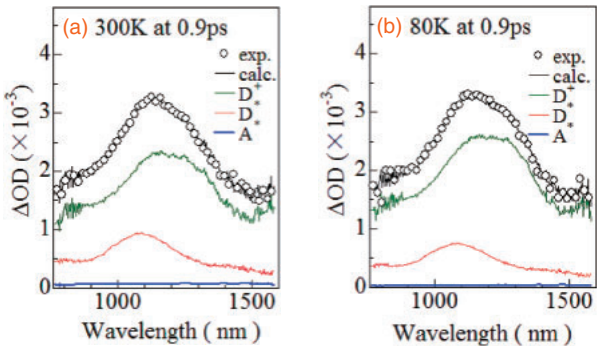

Fig. 3. ΔOD spectra (open circles) of SMDPPEH/$PC_{71}BM$ blend film at (a) 300 K and (b) 80 K, together with the spectral decomposition into PIAs due to D^+ ($C_{D^+}\phi_{D^+}$), D^* ($C_{D^*}\phi_{D^*}$), and A^* ($C_{A^*}\phi_{A^*}$).

described in the literature.[10] The blend film was placed on the cold head of a cryostat, the temperature of which was controlled using liquid nitrogen. As the light source, we employed a regenerative amplified Ti:sapphire laser with a pulse width of 100 fs and repetition rate of 1000 Hz. The 400 nm excitation pulse was generated as second harmonics in a β-BaB_2O_4 (BBO) crystal. The excitation intensity was 27–36 $\mu J/cm^2$. The frequency of the pump pulse was decreased to half (500 Hz) to obtain the "pump-on" and "pump-off" conditions. A white probe pulse (800–1600 nm), generated by self-phase modulation in a sapphire plate, was focused on the sample with the pump pulse. The spots of the pump and probe pulses were 5 and 3 mm in diameter, respectively. The transmitted probe spectra were detected using a 256 ch InGaAs photodiode array attached to a 30 cm imaging spectrometer. The spectral data were accumulated for 20000 pulses to improve the signal/noise ratio. The differential absorption spectrum (ΔOD) is expressed as $\Delta OD \equiv -\log(I_{on}/I_{off})$, where I_{on} and I_{off} are the transmitted light intensity with and without pump excitation, respectively. The time resolution of the system was ~0.2 ps.

Figure 1 shows ΔOD spectra of (a) SMDPPEH and (b) $PC_{71}BM$ neat films. In the neat SMDPPEH film [Fig. 1(a)], the broad absorption band at ≈1100 nm is ascribed to the PIA due to D^*. In the neat $PC_{70}BM$ film [Fig. 1(b)], the structureless absorption extending above ~800 nm is ascribed to the PIA due to A^*. We confirmed that the spectral shape remains unchanged even at 10 ps.

Figure 2 shows ΔOD spectra of SMDPPEH/$PC_{71}BM$ blend films. At 300 K [Fig. 2(b)], the ΔOD spectra show a broad absorption band, the peak position if which shows a red-shift from ~1100 nm at 1 ps to ~1200 nm at 10 ps. The peak position at 1 ps (≈ 1100 nm) suggests that the spectrum contains a considerable D^* component. The red-shift disappears above 10 ps, and the spectral profile becomes independent of t. Therefore, we ascribed the absorption band ($t \geq 10$ ps) to the PIA due to D^+. In fact, the spectral profile of PIA is similar to that of the electrochemical differential absorption spectra of the SMDPPEH neat film.[22] In the early stage (≤10 ps) after photoexcitation, the PIA signal is considered to originate from the weakly bound state of electrons and holes across the D/A boundary.[27] A similar t-dependent behavior of the ΔOD spectra is observed at 80 K [Fig. 2(c)].

In order to reveal the carrier formation dynamics, we decomposed the PIA (ϕ_{exp}) of the SMDPPEH/$PC_{71}BM$ blend film into the PIA components due to D^+ (ϕ_{D^+}), D^* (ϕ_{D^*}), and A^* (ϕ_{A^*}). We regarded the ΔOD spectra of the SMDPPEH/$PC_{71}BM$ blend film (average between 8 to 10 ps), the SMDPPEH neat (at 1 ps) film, and $PC_{71}BM$ neat (at 1 ps) films as the basis functions ϕ_{D^+}, ϕ_{D^*}, and ϕ_{A^*}, respectively. The spectral weights, i.e., C_{D^+}, C_{D^*}, and C_{A^*}, of the respective components were determined so that they minimize the trial function: $F = \Sigma_i[C_{D^+}\phi_{D^+}(\lambda_i) + C_{D^*}\phi_{D^*}(\lambda_i) + C_{A^*}\phi_{A^*}(\lambda_i) - \phi_{exp}(\lambda_i)]^2$, where λ_i denotes the respective wavenumbers. The unit of ϕ_{D^+}, ϕ_{D^*}, and ϕ_{A^*} is optical density. F, C_{D^+}, C_{D^*}, and C_{A^*} are functions of t. We found that the average process of ϕ_{D^+} significantly improves the scattering of C_{D^+}, C_{D^*}, and C_{A^*} against t, which enables us to discuss the difference in τ_{rise} of D^+ and τ_{decay} of D^* and A^*. Figure 3(a) shows a prototypical example of the spectral decompositions at 300 K. We observed that the 400 nm excitation excites both D^* and A^*.

To evaluate the absolute numbers of the donor (n_{D^*}) and acceptor (n_{A^*}) excitons per absorbed photon spectroscopically, we need the absolute intensities of the PIAs per unit density of D^* and A^*. We assumed that one absorbed photon creates one D^* (A^*) in the SMDPPEH ($PC_{71}BM$) neat film. Then, the PIA intensity per unit density of D^* (A^*) becomes $\alpha_{exciton} = 0.028$ (0.002) nm^2/exciton on considering the ab-

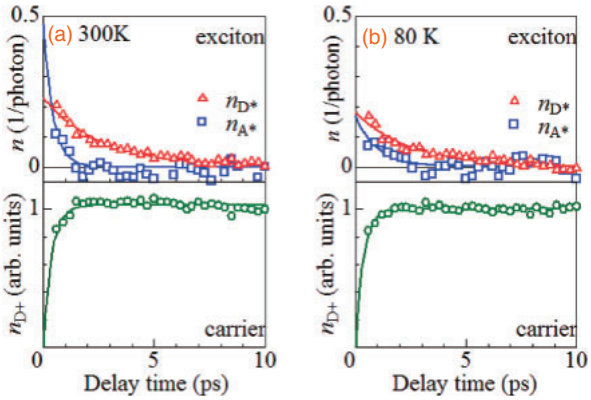

Fig. 4. Absolute number of donor (n_{D^*}) and acceptor (n_{A^*}) excitons per absorbed photon and relative number of donor carriers (n_{D^+}) as functions of the delay time at (a) 300 K and (b) 80 K. Adjacent averages were plotted in n_{A^*}. The solid curves are results of least-squares fittings with exponential functions.

Table I. Characteristic times (τ_{rise} and τ_{decay}) and amplitudes (C) of n_{D^+}, n_{D^*}, and n_{A^*}. The parameters were obtained through least-squares fittings with the exponential function $C(1-e^{-t/\tau_{rise}})$ for n_{D^+} and $Ce^{-t/\tau_{decay}}$ for n_{D^*} and n_{A^*}. The amplitude of D^+ has arbitrary units.

Component	Temperature (K)	τ_{rise} (ps)	τ_{decay} (ps)	C (1/photon)
D^+	300	0.4	—	—
D^+	80	0.4	—	—
D^*	300	—	2.6	0.23
D^*	80	—	2.4	0.18
A^*	300	—	0.4	0.47
A^*	80	—	1.0	0.17

sorption index. Then, n_{D^*} (n_{A^*}) can be calculated by $\alpha_{photon}/\alpha_{exciton}$, where α_{photon} is the PIA intensity of the D^* (A^*) component perunit photon density in the SMDPPEH/$PC_{71}BM$ blend film. Note that we should convert the unit of the D^* (A^*) component from optical density to nm^2/photon by considering the excitation pulse energy and absorption index.

In the upper panel of Fig. 4(a), we plotted the obtained n_{D^*} and n_{A^*} as functions of t at 300 K. In the lower panel of Fig. 4(a), we plotted the relative number of n_{D^+}. We plotted adjacent averages in n_{A^*} because n_{A^*} significantly scatters owing to the small coefficient ($\alpha_{exciton} = 0.002\,nm^2$/exciton) between the PIA and exciton density. The solid curves are results of least-squares fittings with the exponential function $C(1-e^{-t/\tau_{rise}})$ for n_{D^+} and $Ce^{-t/\tau_{decay}}$ for n_{D^*} and n_{A^*}. In the analysis of n_{D^+}, we use a single exponential function without distinguishing the two process, i.e., $D^* \rightarrow D^+$ and $A^* \rightarrow D^+$. The obtained characteristic times (τ_{rise} and τ_{decay}) and amplitudes (C) for D^+, D^*, and A^* are listed in Table I. We found that τ_{rise} (= 0.4 ps) of D^+ is comparable with τ_{decay} (= 0.4 ps) of A^*, indicating that the $A^* \rightarrow D^+$ conversion process is completed within ≈0.4 ps. We note that τ_{rise} (= 0.4 ps) of D^+ of the SMDPPEH/$PC_{71}BM$ blend film is comparable to that (= 0.2–0.3 ps[10]) of the PTB7/$PC_{71}BM$ blend film. The sub-picosecond τ_{rise} observed in the BHJ layer is ascribed to molecular mixing[18–20] as well as the nano-size domain structure.[21]

Our careful analysis revealed that τ_{decay} (= 2.6 ps) of D^* is much greater than τ_{rise} (= 0.4 ps) of D^+. The longer decay time indicates that the late decay component ($t \geq \tau_{rise}$) of D^* does not contribute to the carrier formation process. In other words, the exciton dissociation efficiency steeply decreases with t. This is probably because the excess energy[28] of excitons, which is indispensable to compensate for the coulombic binding energy between the electron and hole, steeply decreases with exciton migration within the domain. The excitons that reach the D/A interface after the long migration have no excess energy to separate into electrons and holes. Then, only the excitons created near the D/A interface contribute to the carrier formation process. Such a hot exciton picture is theoretically supported.[29,30]

Now, let us proceed to the effects of temperature on the carrier formation dynamics. Figure 4(b) shows n_{D^*}, n_{A^*}, and n_{D^+} as functions of t at 80 K. The solid curves are results of least-squares fittings with exponential functions. The obtained τ_{rise}, τ_{decay}, and C for D^+, D^*, and A^* are listed in Table I. We emphasize that τ_{rise} (= 0.4 ps) of D^+ shows no temperature dependence, even though τ_{decay} of A^* significantly increased from 0.4 ps at 300 K to 1.0 ps at 80 K. The effect of temperature on τ_{decay} of A^* is understood in terms of the thermally activated exciton diffusion.[31] The fast τ_{decay} of A^* at 300 K is ascribed to the fast exciton diffusion and resultant additional recombination process at the trap state. The temperature independence of τ_{rise} is well explained if only the excitons created near the interface contribute to the carrier formation process. In this case, τ_{rise} is hardly influenced by temperature because the process is free from activation-type exciton diffusion.

In summary, we spectroscopically clarified the effects of temperature on the carrier formation and exciton decay dynamics in SMDPPEH/$PC_{71}BM$ blend film. We found that τ_{rise} (= 0.4 ps) of D^+ is independent of temperature. The temperature independence suggests that only the excitons created near the D/A boundary contribute to the carrier formation process.

Acknowledgment This work was supported by the Futaba Electronics Memorial Foundation.

1) M. Hiramoto, H. Fujiwara, and M. Yokoyama, Appl. Phys. Lett. **58**, 1062 (1991).
2) N. S. Sariciftci, L. Smilowitz, A. H. Heeger, and F. Wudl, Science **258**, 1474 (1992).
3) I.-W. Hwang, D. Moses, and A. J. Heeger, J. Phys. Chem. C **112**, 4350 (2008).
4) J. Guo, H. Ohkita, H. Benten, and S. Ito, J. Am. Chem. Soc. **131**, 16869 (2009).
5) J. Guo, H. Ohkita, H. Benten, and S. Ito, J. Am. Chem. Soc. **132**, 6154 (2010).
6) K. Yonezawa, M. Ito, H. Kamioka, T. Yasuda, L. Han, and Y. Moritomo, Adv. Opt. Technol. **2012**, 316045 (2012).
7) R. A. Marsh, J. M. Hodgkiss, S. Albert-Seifried, and R. H. Friend, Nano Lett. **10**, 923 (2010).
8) J. M. Szarko, J.-C. Guo, B. S. Rolczynski, and L. X. Chen, J. Mater. Chem. **21**, 7849 (2011).
9) B. S. Rolczynski, J. M. Szarko, H. J. Son, Y. Liang, L. Yu, and L. X. Chen, J. Am. Chem. Soc. **134**, 4142 (2012).
10) K. Yonezawa, H. Kamioka, T. Yasuda, L. Han, and Y. Moritomo, Jpn. J. Appl. Phys. **52**, 062405 (2013).
11) K. Yonezawa, H. Kamioka, T. Yasuda, L. Han, and Y. Moritomo, Appl. Phys. Lett. **103**, 173901 (2013).
12) T. Akaba, K. Yonezawa, H. Kamioka, T. Yasuda, L. Han, and Y.

Moritomo, Appl. Phys. Lett. **102**, 133901 (2013).
13) K. Yonezawa, H. Kamioka, T. Yasuda, L. Han, and Y. Moritomo, Appl. Phys. Express **5**, 042302 (2012).
14) J. Guo, Y. Liang, J. Szarko, B. Lee, H.-J. Son, B. S. Rolczynski, L. Yu, and L. X. Chen, J. Phys. Chem. B **114**, 742 (2010).
15) Y. Liang, Y. Wu, D. Feng, S.-T. Tsai, H.-J. Son, G. Li, and L. Yu, J. Am. Chem. Soc. **131**, 56 (2009).
16) Y. Liang, Z. Xu, J. Xia, S.-T. Tsai, Y. Wu, G. Li, C. Ray, and L. Yu, Adv. Energy Mater. **22**, E135 (2010).
17) Z. He, C. Zhong, S. Su, M. Xu, H. Wu, and Y. Cao, Nat. Photonics **6**, 593 (2012).
18) B. A. Collins, Z. Li, J. R. Tumbleston, R. Gann, C. R. McNeill, and H. Ade, Adv. Energy Matter. **3**, 65 (2013).
19) Y. Moritomo, T. Sakurai, T. Yasuda, Y. Takeichi, K. Yonezawa, H. Kamioka, H. Suga, Y. Takahashi, Y. Yoshida, N. Inami, K. Mase, and K. Ono, Appl. Phys. Express **7**, 052302 (2014).
20) Y. Moritomo, T. Yasuda, K. Yonezawa, T. Sakurai, Y. Takeichi, H. Suga, Y. Takahashi, N. Inami, K. Mase, and K. Ono, Sci. Rep. **5**, 9483 (2015).
21) G. J. Hedley, A. J. Ward, A. Alekseev, C. T. Howells, E. R. Martins, L. A. Serrano, G. Cooke, A. Ruseckas, and I. D. W. Samuel, Nat. Commun. **4**, 2867 (2013).
22) Y. Moritomo, K. Yonezawa, and T. Yasuda, Appl. Phys. Lett. **105**, 073902 (2014).
23) R. A. Marcus, Rev. Mod. Phys. **65**, 599 (1993).
24) S. Qu and H. Tian, Chem. Commun. **48**, 3039 (2012).
25) A. B. Tamayo, B. Walker, and T.-Q. Nguyen, J. Phys. Chem. C **112**, 11545 (2008).
26) A. B. Tamayo, X.-D. Dang, B. Walker, J. Seo, T. Kent, and T.-Q. Nguyen, Appl. Phys. Lett. **94**, 103301 (2009).
27) Y. Moritomo, K. Yonezawa, and T. Yasuda, Sci. Rep. **5**, 13648 (2015).
28) S. D. Dimitrov, A. A. Bakulin, C. B. Nielsen, B. C. Schroeder, J. Du, H. Bronstein, I. McCulloch, R. H. Friend, and J. R. Durrant, J. Am. Chem. Soc. **134**, 18189 (2012).
29) H. Tamura and I. Burghardt, J. Am. Chem. Soc. **135**, 16364 (2013).
30) M. Huix-Rotllant, H. Tamura, and I. Burghardt, J. Phys. Chem. Lett. **6**, 1702 (2015).
31) O. V. Mikhnenko, F. Cordella, A. B. Sieval, J. C. Hummelen, P. W. M. Blom, and M. A. Loi, J. Phys. Chem. B **112**, 11601 (2008).